Am J Cancer Res 2019;9(12):2618-2633
www.ajcr.us /ISSN:2156-6976/ajcr0102924

Original Article

DcR3 promotes proliferation and invasion of pancreatic cancer via a DcR3/STAT1/IRF1 feedback loop

Yijun Wei[1,2*], Xingyu Chen[4*], Jian Yang[1,2], Jun Yao[1,2], Ni Yin[3], Zixiang Zhang[1,2], Dechun Li[1,2], Dongming Zhu[1,2], Jian Zhou[1,2]

[1]Pancreatic Disease Research Centre, Departments of [2]General Surgery, [3]Oncology, The First Affiliated Hospital of Soochow University, Suzhou 215006, Jiangsu, China; [4]Taizhou Fourth People's Hospital, Taizhou 225300, Jiangsu, China. [*]Equal contributors.

Received September 28, 2019; Accepted November 21, 2019; Epub December 1, 2019; Published December 15, 2019

Abstract: Pancreatic cancer (PC) is one of the most common gastrointestinal malignancies that are highly aggressive with a low 5-year survival rate. Accumulated evidence has indicated that decoy receptor 3 (DcR3) is involved in several pathologic processes and various cancers. However, the mechanisms underlying dysregulated DcR3 expression and activation in PC remain to be fully established. In this study, we investigate the function and regulatory network of DcR3 in PC. We found that DcR3 was upregulated in PC tissues and serum. High DcR3 expression was associated with aggressive clinicopathological features and poor prognosis. Functionally, DcR3 not only increased cell migration and invasion in vitro but also promoted tumour growth both in vitro and in vivo by loss-of-function and gain-of-function experiments. Mechanistically, DcR3 promoted the phosphorylation of signal transducers and activators of transcription 1 (STAT1), leading to a dramatic increase in interferon regulatory factor 1 (IRF1). IRF1 then increased the transcriptional activity of DcR3, forming a positive feedback loop to reinforce DcR3 expression. In addition, DcR3 promoted carcinoembryonic antigen-related cell adhesion molecule 1 (CEACAM1) expression through activated IRF1. In conclusion, our findings provided novel insights into the function and mechanism of DcR3 in the pathogenesis of PC, which may be a potential therapeutic target for PC.

Keywords: DcR3, pancreatic cancer, tumorigenesis, STAT1, IRF1

Introduction

Pancreatic cancer (PC) is one of the most common gastrointestinal malignancies in the world and is recognized as the fourth leading cause of cancer-related deaths [1]. In most patients, PC is diagnosed at locally advanced or distant metastatic disease stages, losing the opportunity for surgical resection [2]. Despite recent strides in chemotherapy and targeted therapy, successful therapeutic strategies for PC are limited and the 5-year survival rate remains at only 6%-8% [3]. Invasion and metastasis are the most important characteristics of PC. Therefore, there is an acute need to explore the molecular mechanisms involved in these processes.

Recently, the secretome has gained increased attention in areas of tumourigenesis, metastasis and drug resistance [4, 5]. Pancreatic cancer cells can produce a large amount of secreted proteins into conditioned medium, promoting extracellular matrix (ECM) degradation and tumour cell invasion [6]. These tumour-specific proteins are significant in many cellular functions, including signal transduction and crosstalk with plasma membranes [7, 8].

Decoy receptor 3 (DcR3), also known as tumour necrosis factor receptor superfamily member 6B (TNFRSF6B) or M68, is a secreted molecule because it lacks a transmembrane sequence [9]. A growing volume of literature has reported that DcR3 expression is positively correlated with malignant processes and poor survival in lung cancer [10, 11], gastric cancer [12], pancreatic cancer [13, 14], and colon cancer [15, 16]. Overexpression of DcR3 may contribute to tumour growth and immune suppression by blocking the regulating effects of FasL [17], TL1A [18] and LIGHT [19]. Our previous study

demonstrated that DcR3 protected pancreatic cancer cells from FasL-induced cell apoptosis [20]. A recent study reported that DcR3 induced epithelial-mesenchymal transition (EMT) in colorectal cancer [21]. However, the factors that contribute to its upregulation and the key roles of protein interaction networks in PC remain unknown.

In the present study, overexpression of DcR3 was detected in both the tumour tissues and sera of pancreatic cancer patients and correlated with overall survival. We also found that DcR3 promoted the growth and invasion both in vitro and in vivo and plays a critical role in the phosphorylation of STAT1 and STAT2. DcR3/STAT1/IRF1 formed a positive feedback loop, leading to increased transcriptional activity of DcR3 and CEACAM1, providing a potential therapeutic target for pancreatic cancer.

Materials and methods

Patients and samples

A total of 112 serum samples were obtained from pancreatic cancer patients (stage: I, 28; II, 36; III, 26; IV, 22) at First Affiliated Hospital of Soochow University from September 2012 to December 2015. Forty serum samples of healthy volunteers were recruited as controls for this study. Pancreatic cancer tissues and paired adjacent non-tumourous tissues were obtained from 64 patients who underwent surgery for pancreatic cancer (stage I and II). All of the resected and needle biopsy samples were confirmed by diagnostic pathology. No local or systemic neoadjuvant radiotherapy and/or chemotherapy and targeted therapy were managed. Tumour grade was classified according to the World Health Organization (WHO) criteria, and the patients were staged according to the 8th edition of the American Joint Committee of Cancer (AJCC) staging system. Informed consent was obtained from all of the patients, and the study was approval by the Ethics Committee of Soochow University.

Reagents

Antibodies were obtained from the following sources. The antibodies against DcR3 (Ab-57956), CEACAM1 (Ab108397) and CDH11 (Ab151302) were purchased from Abcam (Cambridge, UK). Antibodies against phospho-STAT1 (9167s), phospho-STAT2 (4441s), phospho-STAT3 (9145), STAT1 (9172s), STAT2 (4594s), and STAT3 (9139) were from Cell Signaling Technology (MA, USA). Anti-IRF1 (11335-1-AP) was obtained from Proteintech (IL, USA). GAPDH was from Multi Sciences. Horseradish peroxidase-conjugated goat anti-mouse IgG and goat anti-rabbit IgG were obtained from Solarbio (Beijing, China).

Fludarabine, a STAT1 activation inhibitor, was purchased from Selleck (TX, USA), dissolved in DMSO and used to treat cells for 48 hours at 2.5 μM.

Cell culture

The human pancreatic cancer cell lines SW1990, PL45, PATU8988, CFPAC-1, and PANC-1 were obtained from the Chinese Academy of Sciences (Shanghai, China). All of the cells were cultured in Dulbecco's Modified Eagle Medium (DMEM; HyClone, UT, USA) containing 10% foetal bovine serum (Gibco, NY, USA) in 5% CO_2 at 37°C.

Plasmids, small interfering RNAs and transfection

Expression vectors encoding DcR3 were constructed by cloning the open reading frames and downstream 3'-UTR into the pcDNA3.1 vector (Invitrogen, CA, USA) (OE-DcR3). The empty pcDNA3.1 vector served as a negative control (Vector). The siRNA sequence targeting DcR3 was designed and synthesized by GenePharma (Suzhou, China). The siRNA sequence targeting DcR3 (si-DcR3) was 5'-CUCAAUGUGCCAGGCUCUUTT-3'. A nonspecific scrambled siRNA sequence (si-Scramble) was used as a negative control (5'-UUCUCCGAAGGUGUCACGUTT-3').

PATU8988 and PL45 cells were transfected with plasmids or siRNA using Lipofectamine 2000 (Invitrogen, CA, USA) according to the manufacturer's protocol. Cells were incubated for 48 h before use in experiments.

Cell proliferation

A cell proliferation assay was performed with the cell-counting kit-8 (CCK8, Dojindo, Japan). In total, 5×10^3 cells were seeded per well in 96-well culture plates with 100 μL complete medium. Then, 10 μL CCK8 was added to each well, and the plates were cultivated at 37°C for

2 hours with 5% CO_2. Then, the absorbance at 450 nm was read using a 96-well microplate reader (Scientific Multiskan MK3, Thermo Finland). The cell proliferation assay was performed at 0, 24, 48, and 72 hours.

Clone formation assay

Cells were seeded into 6-well plates in a density of 500 cells/well. The media were changed every 2 days, and the cells were allowed to grow for 14 days. Cells were fixed with 4% paraformaldehyde and stained with 1% crystal violet. Cell colonies containing at least 20 cells were counted using an inverted microscope at 40× magnification.

Wound healing assay

Cells were seeded into 6-well plates in a density of 3×10^5 cells/ml and cultured. When the cells were confluent, three scratches were made in each well using a 10-μl pipette tip. After washing away the detached cells by sterile PBS, cells were cultured in medium supplemented with 2% FBS under standard condition. At 0, 24, 48 and 72 h after scratch, images of the wounds were captured for the measurement of wound width.

Cell invasion assays

Cell invasion assays were performed using Transwell® cell culture chambers with 8 μm pores (Corning, NY, USA). The inserts in the membrane filter were coated with 40 μl configured Matrigel™ on the upper surface. The cells were resuspended in serum-free DMEM at a concentration of 5×10^5 cells/ml and placed in the upper chamber. The lower chamber was filled with DMEM with 10% FBS. After incubation at 37°C for 48 hours, the invading cells at the bottom of the Matrigel™ were fixed in methanol and stained with 0.1% crystal violet. The number of invading cells in five random fields per well was calculated using a microscope at 200× magnification.

Microarray and data analysis

Si-DcR3 (n=3) and si-Scramble cells (n=3) were collected for total RNA isolation. Then the extracted RNA samples were assayed for genome-wide expression changes by an Affymetrix GeneChip array (Thermo Fisher Scientific, MA, USA) following the manufacturer's instructions. All RNA samples were processed three times to generate a technical replicate. The filtration was performed by comparing the gene expression levels between si-DcR3 and si-Scramble cells. Differential genes were selected based on P value <0.05 and absolute fold change >2. Functional enrichment analysis was performed using Blast2GO, and GO annotation was applied to describe the functions of the differentially expressed genes. Moreover, the ingenuity pathway analysis (IPA) software was used to assign differentially expressed genes to specific biological functions and pathways which related to DCR3 gene.

Western blot

Proteins were extracted using lysis buffer and quantified by bicinchoninic acid (BCA) protein quantitative assay (KeyGen Biotech, Nanjing, China). Protein lysates were separated using 10% SDS-PAGE and then transferred onto PVDF membranes (Roche, Switzerland). Then, the membranes were incubated with primary antibodies (DcR3, CEACAM1, CDH11, STAT1, STAT2, STAT3, IRF1, and phospho-STAT1/2/3 at 1:1000 dilution; GAPDH at 1:5000 dilution) at 4°C overnight, followed by incubation with horseradish peroxidase-conjugated goat anti-mouse IgG (1:5000) or goat anti-rabbit IgG (1:5000). Finally, the membranes were detected using an enhanced chemiluminescence (ECL) detection system (FDbio, China). All experiments were performed according to the manufacturer's instructions.

Chromatin immunoprecipitation assay

Chromatin immunoprecipitation (ChIP) assay was performed using a ChIP assay kit (Upstate Biotechnology, MA, USA) as described by the manufacturer. Briefly, crosslinked chromatin was sonicated into 200 to 1000 bp fragments. Anti-phospho-STAT1 and anti-IRF1 were used to precipitate DNA-protein complexes. Mouse immunoglobulin G (IgG) was used as a negative control. After removing protein and RNA, the ChIP-derived DNA was subjected to polymerase chain reaction (PCR). The primers are listed in Table S1.

Luciferase reporter assay

The IRF1, DcR3 and CEACAM1 promoter regions were cloned into the pGL3-basic pro-

moter vector (Promega, WI, USA). The mutation reporters (separate deletions of binding sites in the promoter) were then generated. Luciferase reporter assays were performed by transfecting the mutated promoter reporter plasmid, together with the pRL-TK vector (Promega), into human HEK293T cells using Lipofectamine 2000 (Invitrogen). After 48 h transfection, luciferase activities were detected using a dual luciferase assay system (Promega) according to the manufacturer's instructions.

Animal experiments

BALB/C nude mice (female, 4-6 weeks old and 16-20 g) were purchased from the Shanghai Experimental Animal Centre (Shanghai, China). All animal experiments were performed in accordance with the Guide for the Care and Use of Laboratory Animals of Soochow University. For xenograft models, an siRNA sequence targeting DcR3 (5'-CGCTGGTTT-CTGCTTGGAGCAC-3') was subcloned into a lentiviral vector (LV-si-DcR3), and a lentiviral vector containing a random sequence was used as a control (LV-si-Ctrl). Full-length DcR3 was synthesized and subcloned into a GV358 vector (Genechem, Shanghai, China), designated LV-DcR3. The empty vectors served as a negative control (LV-Ctrl). To study cell growth in vivo, 5×10^6 cells were injected subcutaneously into the right flank of nude mice (n=5 per group). The tumour-bearing mice were sacrificed when they became moribund or on day 30 after injection and their tumours were removed. Tumour dimension was determined by calliper measurements of the length and width. Tumour volume was calculated using the following formula: tumour volume = (length × width^2)/2.

Immunohistochemistry

Tissues were fixed with formalin and embedded in paraffin. According to the specifications of the S-P (streptavidin peroxidase) kit, 4 μm thick sections were retrieved with citrate buffer, incubated with anti-DcR3 (1:200), anti-CEACAM1 (1:1000), anti-phospho-STAT1 (1:200) and anti-IRF1 (1:300) monoclonal antibodies overnight at 4°C, followed by incubation with the secondary antibody and ExtrAvidin-conjugated horseradish peroxidase. Sections were evaluated by light microscopy and staining intensity was scored semi-quantitatively by multiplication of the intensity score (0, negative; to 1, low; 2, medium; or 3, high) and the quantity score (0 for ≤ 5%; 1, 6% to 25%; 2, 26% to 50%; 3, 51% to 75% and 4 for >75%). Scores of six of more were considered to represent positive expression.

ELISA

The level of DcR3 in human serum was measured using a commercially available sandwich ELISA kit (R&D, MS, USA). Procedures were conducted as suggested by the manufacturer.

Statistical analysis

Statistical analysis was performed using SPSS version 19.0 software. All numerical data are presented as the means ± S.D. for multiple samples, except for the relative DcR3 level in patients, which is presented as median with range. Mann-Whitney test was used for non-parametric variables, and parametric variables were compared using one-way analysis of variance (ANOVA) or t-test. Categorical variables were compared by Chi square test. The correlation analysis was performed using a Spearman's Rank Correlation test. Survival was assessed according to the Kaplan-Meier method and compared using the log-rank test. Differences were considered significant at values of $P<0.05$.

Results

DcR3 is upregulated in PC and its expression correlates with prognosis

We first analysed the RNA-seq data of pancreatic cancer from the Cancer Genome Atlas (TCGA). The results indicated that transcripts per million (TPM) of DcR3 were significantly elevated in PC tissues compared with matched normal tissues (P<0.001, **Figure 1A**). Moreover, PC patients with high TPM of DcR3 exhibit significantly shorter overall survival than patients with low DcR3 TPM (P=0.013, **Figure 1B**).

We also detected the serum levels of DcR3 in 112 cases of PC in The First Affiliated Hospital of Soochow University. The results confirmed that the serum DcR3 was upregulated in patients with PC compared to control subjects (P<0.001, **Figure 1C**). Similarly, assessment via

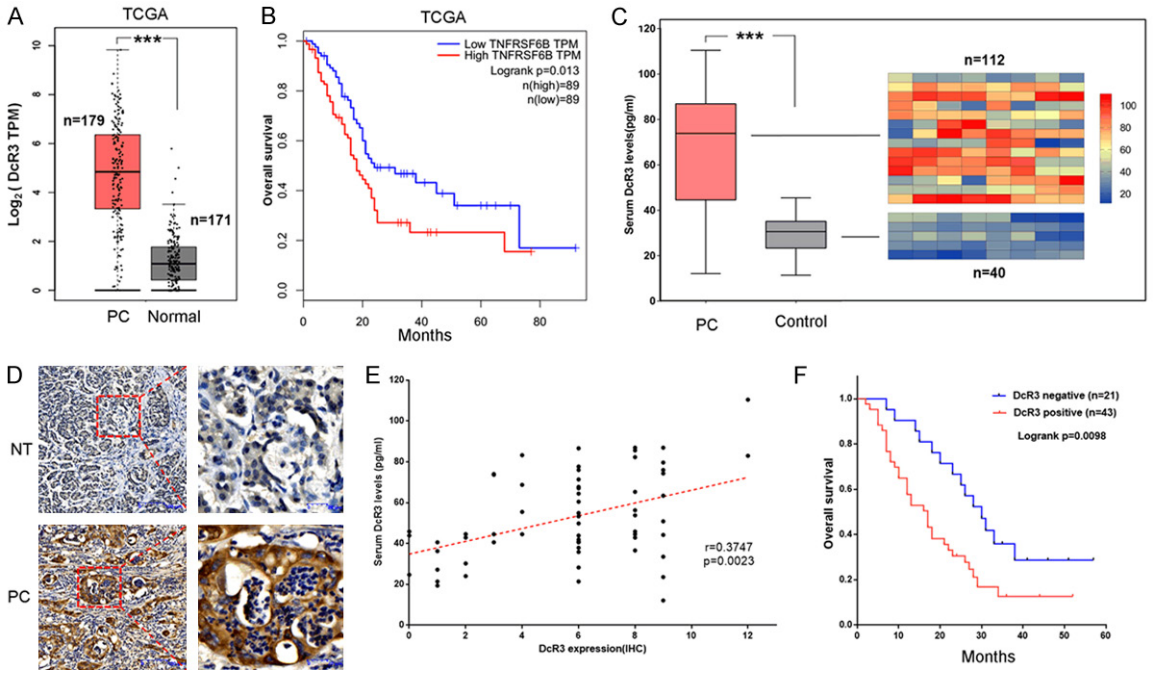

Figure 1. DcR3 is upregulated in PC and its expression correlates with prognosis. (A) DcR3 is significantly elevated in PC tissues (n=179) compared with normal tissues (n=171) obtained from TCGA database (***P<0.001). (B) Kaplan-Meier curve of low DcR3 (n=89) and high DcR3 (n=89) expression patients from TCGA database (P=0.013) were evaluated using the log-rank test. (C) The serum DcR3 level of PC patients (n=112) was higher than that of the control group (n=40) (***P<0.001). Mann-Whitney test was used to analyze the differences between groups in (A and C), data were presented as the median with range. (D) Immunohistochemistry (IHC) staining indicated that DcR3 expression is upregulated in human pancreatic cancer tissues compared with non-tumour pancreatic tissues (NT) (left panel: magnification ×100; right panel: magnification ×400) (χ^2=19.574, ***P<0.001). (E) The positive relationship was observed between DcR3 serum concentrations measured by ELISA and DcR3 expression by IHC (P=0.023). (F) Kaplan-Meier curves of pancreatic cancer patients with negative (n=21) versus positive (n=43) expression levels of DcR3 were evaluated using the log-rank test, P=0.098.

IHC revealed that DcR3 was overexpressed in PC tissues (n=64) compared with adjacent non-tumour pancreatic tissues (χ^2=19.574, P<0.001, **Figure 1D**). Examination of the correlation between DcR3 and clinical pathological features revealed that DcR3 overexpression was correlated with larger tumour size (P=0.040), lymph node metastasis (P=0.037) and advanced clinical stage (P=0.010) (**Table 1**). Moreover, the serum levels of DcR3 were associated with DcR3 expression as determined by IHC in the tumour tissues (r=0.3747, P=0.0023, **Figure 1E**). These samples of PC were classified into a DcR3 negative group (n=21) and a DcR3 positive group (n=43) determined by immunostaining. Consistent with the TCGA database, patients with DcR3 positive expression were associated with shorter overall survival (P=0.0098, **Figure 1F**). Collectively, these data suggested that DcR3 was overexpressed in both tumour tissues and serum of pancreatic cancer patients and correlated with overall survival.

Regulation of DcR3 expression in pancreatic cancer cells

We detected and compared the expression level of DcR3 protein in five pancreatic cancer cell lines, including CFPAC-1, SW1990, PANC-1, PL45 and PATU8988, by Western blot. From the results, we found that PATU8988 cells had the highest expression of DcR3 in contrast with the PL45 cells, which expressed a low level (**Figure 2A**). To evaluate the effects of DcR3 on the biological behaviour of pancreatic cancer cells, we manipulated the expression of DcR3 by transfecting DcR3 cDNA into PL45 cells or DcR3 siRNA into PATU8988 cells. Western blot confirmed that DcR3 expression was upregulated (P<0.0001) or downregulated (P<0.01), compared with that observed in controls (**Figure 2B**).

Table 1. Relationship between DcR3 expression and clinical pathological features of PC patients

Features	Cases	DcR3		χ^2	*P* value
		positive	negative		
Gender					
Male	31	20	11	0.194	0.659
Female	33	23	10		
Age (years)					
≤ 65	25	18	7	0.431	0.512
>65	39	25	14		
Tumor location					
Head	37	24	13	0.215	0.643
Body and tail	27	19	8		
Tumor size (cm)					
≤ 4	34	19	15	4.205	0.040*
>4	30	24	6		
Differentiation					
Well/Moderate	35	27	8	3.472	0.062
Poor	29	16	13		
Lymph node metastasis					
N	37	21	16	4.328	0.037*
Y	27	22	5		
Clinical stage					
I	28	14	14	6.670	0.010*
II	36	29	7		

*$P<0.05$.

DcR3 promoted proliferation, migration and invasion of pancreatic cancer cells in vitro and in vivo

A CCK8 assay revealed that cell growth was significantly impaired in PATU8988 cells transfected with si-DcR3 (P<0.05 for 24 h; P<0.0001 for 48 h, 72 h) while the upregulation of DcR3 expression in the PL45 cells promoted cell growth compared with the vector group (P<0.0001 for 24 h, 48 h, 72 h, **Figure 2C**). A similar trend was observed in a colony formation assay as enhanced DcR3 expression in PL45 cells promoted cell proliferation (P<0.0001, **Figure 2D**). Conversely, transfection of PATU8988 cells with si-DcR3 impeded the colony forming efficiency by approximately 50% (P<0.0001). To investigate whether DcR3 contributes to tumor growth in vivo, we established xenografts in nude mice using lentivirus-mediated PATU8988 cells with stably silenced DcR3 and PL45 cells that stably overexpressed DcR3, as well as the respective empty vectors. After two weeks, there was a dramatic decrease in tumour volume in the si-DcR3 group compared with the control group (P<0.001, **Figure 2E**), whereas DcR3 knockdown in the si-DcR3 group had the opposite effect, suppressing tumor growth (P<0.001).

We investigated the cell migration and invasion ability via wound healing assay and transwell systems respectively, after performing DcR3 ectopic transfection or DcR3 knockdown. We found that the si-DcR3 pancreatic cells with knocked down DcR3 displayed relatively slower migration towards the wound space compared with the si-Scramble cells (P<0.0001, **Figure 2F**). However, the upregulation of DcR3 expression in the OE-DcR3 group could enhance the migration speed towards the wound space (P<0.001). Similar results were observed in the transwell assay showing that DcR3 promoted cell invasion (P<0.001, **Figure 2G**). To further demonstrate the function of DcR3, we performed a rescue experiment for siRNA experiments. We first silenced DcR3 expression by RNAi and then upregulated DcR3 expression by pcDNA3.1-DcR3. Western blot indicated that the co-transfection of pcDNA3.1-DcR3 and si-DcR3 in PATU8988 cells efficiently restored DcR3 expression (P<0.01, Figure S1A). After that, we found that overexpression of DcR3 on the basis of knockdown of DcR3 partially reversed the suppression of proliferation and invasion induced by DcR3 silencing (P<0.01, Figure S1B; P<0.01, Figure S1C). Taken together, these results indicated that DcR3 promoted proliferation, migration and invasion of pancreatic cancer cells in vitro and in vivo.

Pathway and biological interaction network analysis of DcR3 target genes

The above findings indicated that DcR3 is significant for malignant phenotypes in human pancreatic cancer cells. However, mechanisms underlying DcR3's impact on tumour development and its downstream pathways have not been systematically explored. We performed

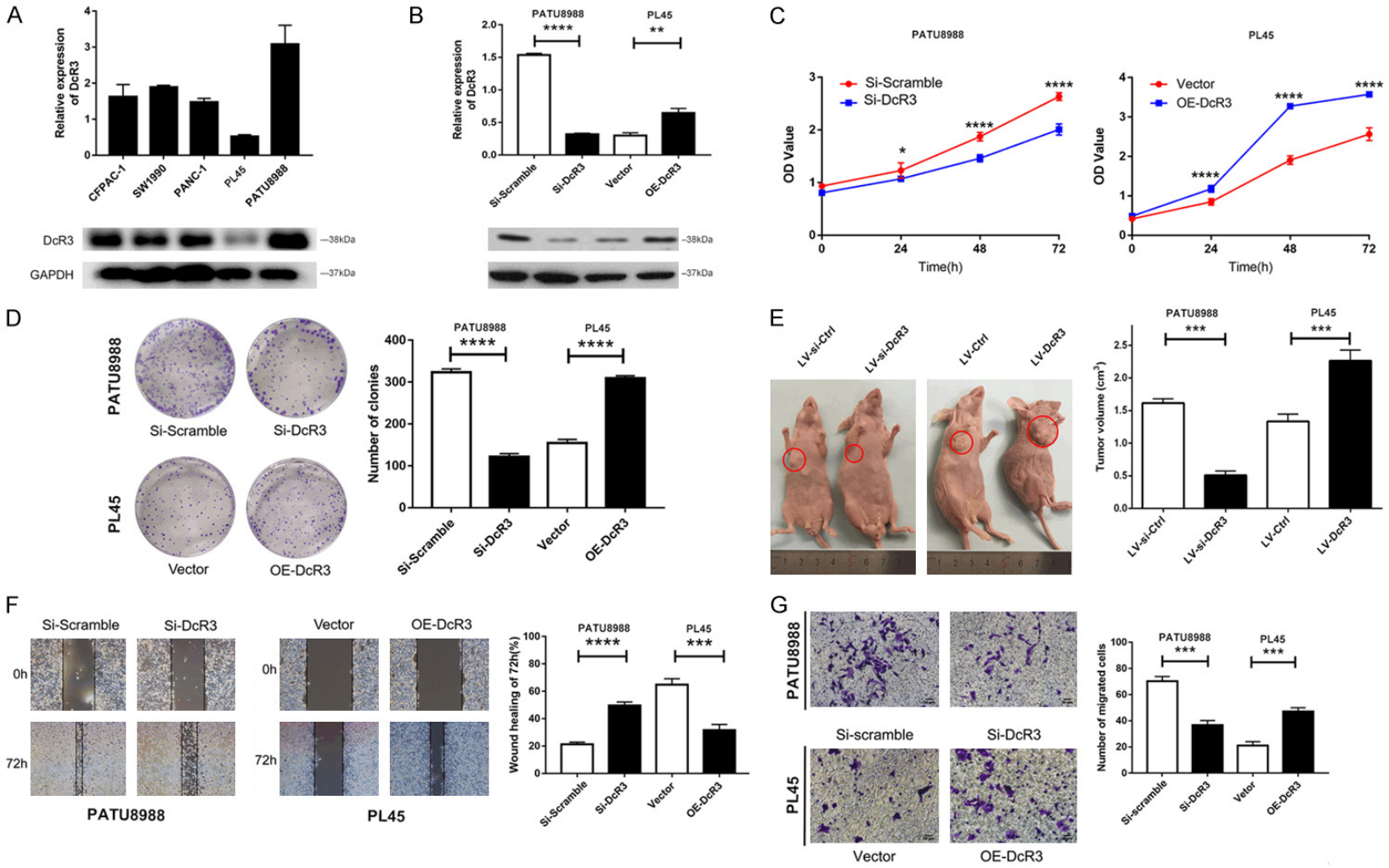

Figure 2. DcR3 is expressed in pancreatic cancer cells and promoted the proliferation, migration and invasion of pancreatic cancer cells in vitro and in vivo. A. The relative expression of DcR3 was examined by Western blot in five PC cell lines (CFPAC-1, SW1990, PANC-1, PL45 and PATU8988). B. DcR3 expression level was increased after transfection with the DcR3 expression plasmid in PL45 cells. DcR3 expression level was suppressed by specific siRNAs in PATU8988 cells. C. Growth curves of PATU8988 and PL45 cells after transfection with si-DcR3 or OE-DcR3 were determined via CCK8 assays. D. The anchorage-independent growth of PATU8988 and PL45 cells was assessed via colony formation assays. E. Four representative Photographs of the pancreatic cancer xenografts from LV-si-DcR3 or LV-DcR3 cells are shown. Histogram shows the mean tumor weights after the tumours harvested. F. The width of the scratch-wounded cell monolayer was recorded at 0 and 72 h after wounding via photography. G. DcR3 promoted PC cell invasion based on Transwell assays. Representative images of migrating cells are shown, scale bars =50 μm. The data were represented as the mean ± S.D. of three independent experiments in vitro or five independent experiments in vivo. Significant differences are indicated as follows: **P*<0.05, ***P*<0.01, ****P*<0.001 and *****P*<0.0001.

microarray analysis comparing the gene expression of si-DcR3 cells and negative control. In total, 868 genes exhibited significant differential expression (P<0.05 and fold change >1.5), including 351 upregulated genes and 517 downregulated genes.

Gene Ontology (GO) analysis indicated that the enrichment of these genes regulated by DcR3 were involved in Biological Process (BP), Cellular Component (CC) and Molecular Function (MF), including regulation of type III interferon production (GO:0034344), host cell (GO:0043657), hydrolase activity (GO:0016817), etc. (P<0.05, Figure S2). Then, Kyoto Encyclopedia of Genes and Genomes (KEGG) enrichment analysis was performed and the differentially expressed genes were enriched in fifteen pathways (P<0.05, **Figure 3A**), including the JAK-STAT signalling pathway (hsa04630), prolactin signalling pathway (hsa04917), Toll-like receptor signalling pathway (hsa04620), etc.

To further clarify the direct and indirect interactions among the identified genes, we performed Ingenuity Pathway Analysis (IPA) to generate a network. The network was centred around STAT1/STAT2, NF-κB, IFN-α/IFN-β, IRF1, and IRF7, which regulate inflammation, cell growth and apoptosis (**Figure 3B**).

DcR3 enhanced the phosphorylation of STAT1

To verify the potential link between STAT1, STAT2 and DcR3 based on the microarray analysis, we detected the phosphorylation levels of STAT1, STAT2 and STAT3 after manipulating DcR3 expression. As shown in **Figure 3C**, upregulation of DcR3 could enhance the phosphorylation levels of STAT1 (P<0.001, **Figure 3D**) and STAT2 (P<0.01, **Figure 3E**), whereas the total STAT1 and STAT2 levels remained unchanged (P>0.05). Downregulation of DcR3 had the opposite effect (P<0.001 for p-STAT1; P<0.01 for p-STAT2), consistent with the microarray analysis findings. In addition, we found that DcR3 had no effect on STAT3 (P>0.05, **Figure 3F**).

To confirm the effect of DcR3 mediated by STAT1, Fludarabine, a STAT1 activation inhibitor, was used to treat OE-DcR3 and negative control cells. After treatment with Fludarabine for 48 h, the phosphorylation of STAT1 was significantly inhibited in OE-DcR3 cells (P<0.001, **Figure 4A**). As shown in **Figure 4B** and **4C**, we found that treatment with Fludarabine partially reversed cell proliferation and invasion promoted by DcR3 expression (P<0.0001). These results indicated that the effect of DcR3 in pancreatic cancer cells could be partially mediated by STAT1 activation.

A positive regulatory loop between DcR3, STAT1 and IRF1

Phosphorylation of STAT1 facilitates nuclear translocation and transcriptional regulation. To further explore the downstream targets of STAT1 in pancreatic cancer, we performed JASPAR database analysis combined with our IPA analysis (**Figure 3B**). Two potential STAT1 protein binding sites were predicted on the promoter regions of the IRF1 gene (**Figure 5A**). ChIP assays showed that STAT1 bound to the IRF1 promoter P1 site but not to the promoter P2 site (**Figure 5B**). A luciferase assay further confirmed that the deletion of P1 in the promoter caused an obvious decrease in luciferase activity compared with a wild type vector (P<0.01, **Figure 5C**). These findings indicated that STAT1 increased the transcriptional activity of IRF1 by binding to the IRF1 promoter P1 site.

To investigate whether DcR3 regulated IRF1 expression through STAT1 phosphorylation, we examined the IRF1 expression in OE-DcR3 cells with or without Fludarabine treatment. As shown in **Figure 5D**, DcR3 enhanced the expression of IRF1 (P<0.01) while Fludarabine largely abolished the DcR3-induced promoting activity on IRF1 (P<0.01). Our data demonstrated that IRF1 was upregulated by DcR3 partially through STAT1 activity.

IRF1 was initially characterized as a transcriptional activator. From the JASPAR database, we examined which genes were the direct transcriptional targets of IRF1. Interestingly, the promoter region of the DcR3 gene was identified as having a potential binding site (-1675 to -1666 bp) for transcription factor IRF1. ChIP analysis of PATU8988 cells using specific antibodies against IRF1 showed occupancy of IRF1 on the DcR3 promoter (**Figure 5E**). Luciferase assays revealed that IRF1-based DcR3 regulation was lost when the region between -1675 and -1666 bp was mutated (P<0.01, **Figure**

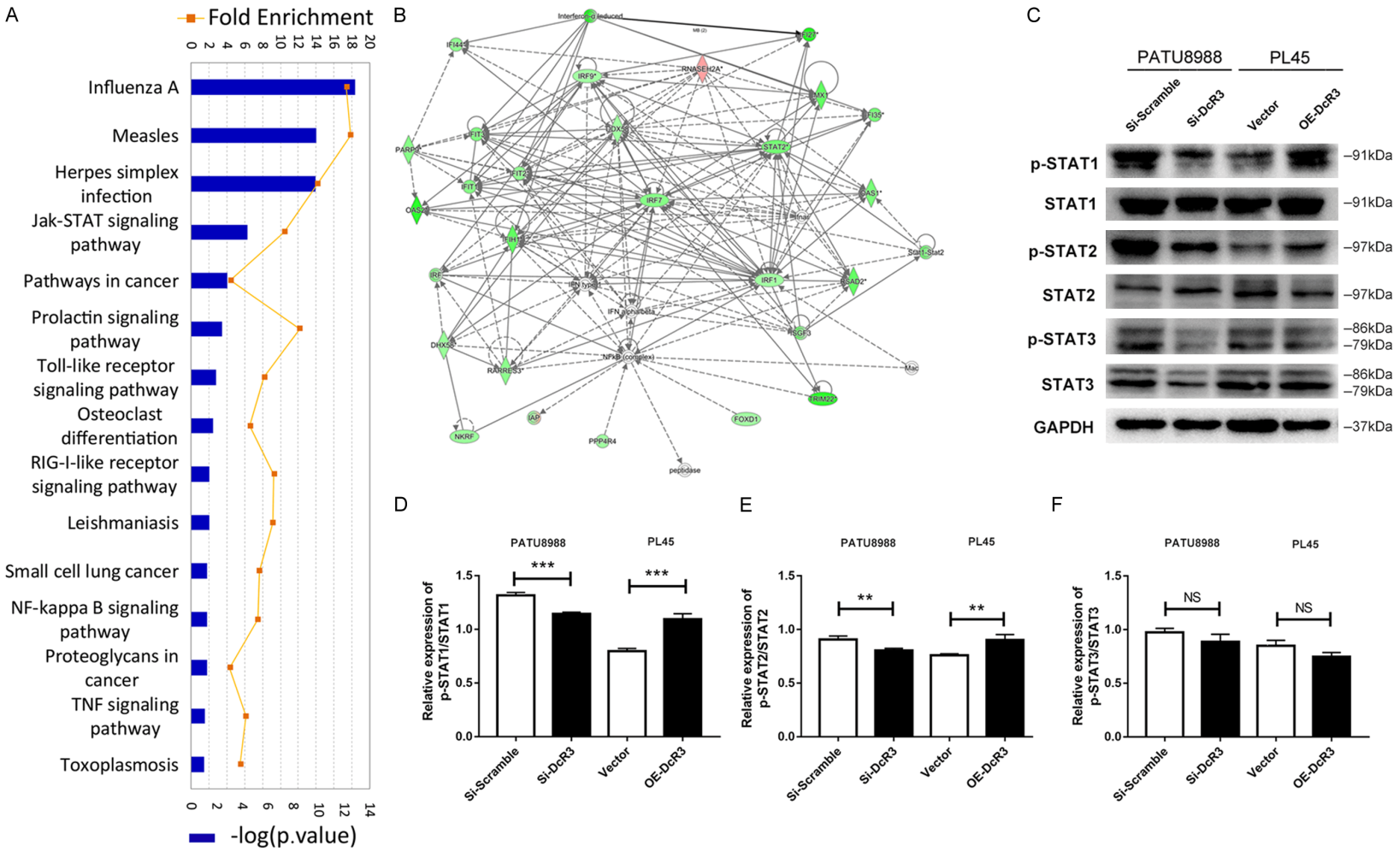

Figure 3. Pathway and biological interaction network analysis of DcR3 target genes and DcR3 enhanced the phosphorylation of STAT1. A. Differentially expressed genes were enriched in fifteen pathways through KEGG enrichment analysis ($P<0.05$). B. The direct and indirect interactions among the identified genes by IPA. C. Western blot assays showed changes in the levels of STAT1, STAT2, STAT3 and their phosphorylation in DcR3 knockdown or DcR3-overexpressing cells. These protein levels were normalized to GAPDH. D-F. Histograms show the relative expression of p-STAT1/STAT1, p-STAT2/STAT2 and p-STAT3/STAT3. The data were represented as the mean ± S.D. of three independent experiments in vitro. Significant differences are indicated as follows: **P<0.01, ***P<0.001.

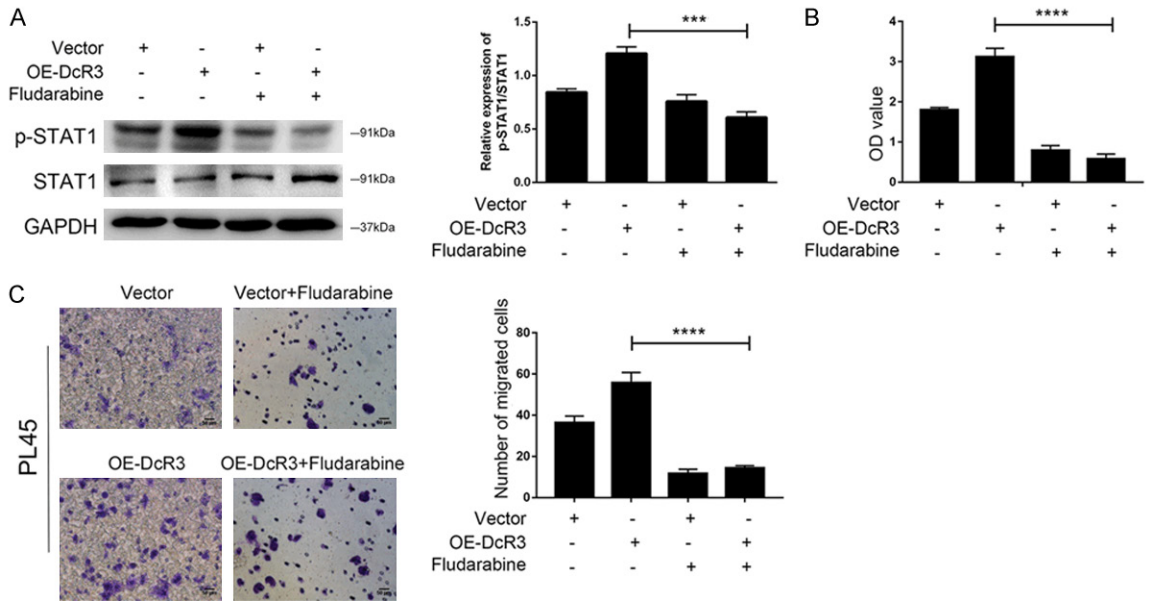

Figure 4. Inhibiting the STAT1 signalling pathway suppressed the proliferation and migration of pancreatic cells. A. OE-DcR3 cells were cultured with 2.5 μM Fludarabine for 48 h. Western blot analyses were performed to evaluate the effects of the inhibitor on phosphorylation levels of STAT1. GAPDH was used as a loading control. Histograms show the relative expression of p-STAT1/STAT1. B. CCK8 assay results demonstrating inhibited proliferation in OE-DcR3 cells treated with 2.5 μM Fludarabine. C. Transwell assays results demonstrating inhibited invasion in OE-DcR3 cells treated with 2.5 μM Fludarabine. The data were represented as the mean ± S.D. of three independent experiments in vitro. Significant differences are indicated as follows: ***P<0.001, ****P<0.0001.

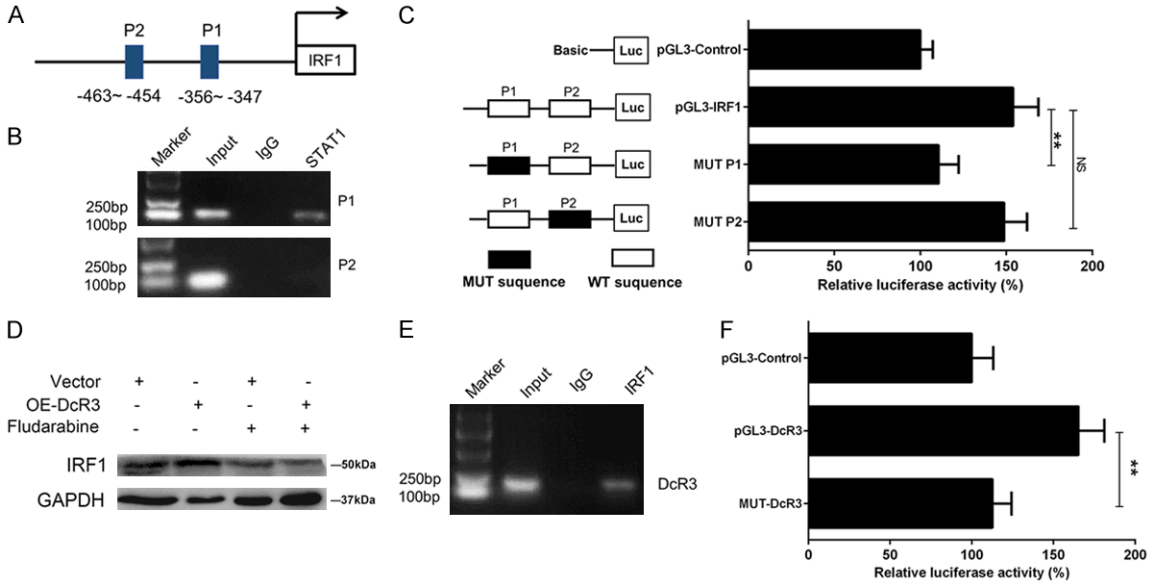

Figure 5. A positive regulatory loop between DcR3, STAT1 and IRF1. A. Prediction of two potential STAT1 protein binding sites for IRF1. B. ChIP assay showed PCR products targeting P1-P2 of the IRF1 promoter. Specific anti-STAT1 or control normal mouse IgG was used for immunoprecipitations, whereas genomic DNA was used as the input control. C. Luciferase assay confirmed that the deletion of P1 (-356~-347 bp) in the promoter caused an obvious decrease in luciferase activity compared with the wild type vector (**P<0.01). D. The relative expression of IRF1 was decreased after the OE-DcR3 cells were treated with Fludarabine (2.5 μM) for 48 hours by Western blot. E. ChIP analysis of PATU8988 cells using specific antibodies against IRF1 showed occupancy of IRF1 on the DcR3 promoter. F. Luciferase assay revealed an obvious decrease in luciferase activity when DcR3's promoter region between -1675 and -1666 bp was mutated (**P<0.01).

5F), validating the ChIP results. Western blot confirmed that IRF1 enhanced DcR3 expression (**Figure 6G**). Therefore, these results demonstrated that DcR3/STAT1/IRF1 formed a positive regulatory loop that is involved in cell proliferation and invasion of pancreatic cancer through increasing DcR3 expression.

DcR3 promoted CEACAM1 expression via transcriptional regulation of IRF1

Plasma membrane proteins are located at the cell surface to interact with secreted proteins. From CC of GO analysis, we found that 8 plasma membrane proteins were regulated by DcR3 (**Figures 6A** and S2). The top three (CEACAM1, CDH11 and TNFRSF10B) were interrogated by TCGA database, which revealed that CEACAM1 and CDH11 were upregulated in pancreatic cancer tissues compared with control ($P<0.001$, **Figure 6B**). However, TNFRSF10B showed no significant difference between the two groups ($P>0.05$). Next, we confirmed our microarray results by Western blot, which indicated that CEACAM1 and CDH11 were correlated with DcR3 (**Figure 6C**). As shown in **Figure 6D**, DcR3 TPM was associated with CEACAM1 TPM ($P=0.037$) but not with CDH11 ($P=0.270$).

Our findings suggested that DcR3/STAT1/IRF1 formed a positive feedback loop and DcR3 promoted CEACAM1 expression. We finally investigated whether IRF1 could regulate the transcriptional activity of CEACAM1. ChIP and luciferase assays showed that IRF1 could bind to the two CEACAM1 promoter sites (**Figure 6E** and **6F**). Western blot confirmed that IRF1 enhanced DcR3 expression (**Figure 6G**), suggesting that IRF1 enhances CEACAM1 expression in pancreatic cancer cells.

Relationship between DcR3/STAT1/IRF1 and CEACAM1 in pancreatic cancer tissues

Finally, to test whether the relationship between DcR3, STAT1, IRF1 and CEACAM1 is clinically relevant, IHC for phosphorylated STAT1 (p-STAT1), IRF1 and CEACAM1 was performed on the 64 pancreatic cancer tissues that were used for DcR3 analysis. We found that DcR3 positive expression tended to correlate with increased expression of p-STAT1, IRF1 and CEACAM1 (**Figure 7A**). Further correlation analysis revealed that the expression of DcR3 was significantly correlated with that of p-STAT1 ($r=0.3904$, $P=0.0014$), IRF1 ($r=0.2998$, $P=0.0161$) and CEACAM1 ($r=0.3523$, $P=0.0043$) (**Figure 7B-D**). These results indicated that the DcR3/STAT1/IRF1 feedback loop and CEACAM1 were active in human pancreatic cancer.

Discussion

In the present study, our experimental and clinical evidence strongly suggested that DcR3 was overexpressed in pancreatic cancer patients, correlated with overall survival, and promoted tumour cell growth and invasion in vitro and in vivo. Additionally, we demonstrated for the first time that DcR3 enhanced the phosphorylation of STAT1 and that the activity of STAT1 stimulated the expression and transcriptional activity of IRF1. DcR3/STAT1/IRF1 formed a positive feedback loop, leading to increased transcriptional activity of DcR3 and CEACAM1 (**Figure 7E**).

Previous studies demonstrated that several solid tumours release large amounts of secreted proteins. Some of these factors are tumour-specific and play crucial roles in the process of tumourigenesis. In cancer patients, elevated serum DcR3 levels correlated with poor prognosis and resistance to chemotherapy [22, 23]. There is accumulating evidence that DcR3 can inhibit cell apoptosis by neutralizing three members of the tumour necrosis factor superfamily (TNFSF): FasL, LIGHT, and TL1A. In addition, DcR3 regulates dendritic cell (DC) differentiation, leading to Th2 polarization and induction of monocyte adhesion [24]. In the present study, we found that DcR3 was upregulated in both tumour tissues and serum of pancreatic cancer specimens. Overexpression of DcR3 promoted tumour cell growth and invasion, whereas knockdown of DcR3 expression produced opposite results.

Multiple signalling pathways, including TGF-β3/SMAD [21], PI3K/Akt [12] and NF-κB [25], are activated downstream of DcR3 in human tumours. However, the pathways that contribute to DcR3 and the molecular and functional interaction in pancreatic cancer have remained unclear. In the current study, we performed microarray analysis comparing the gene expression of DcR3 knockdown cells and negative control. Our data indicate that, first, the JAK-

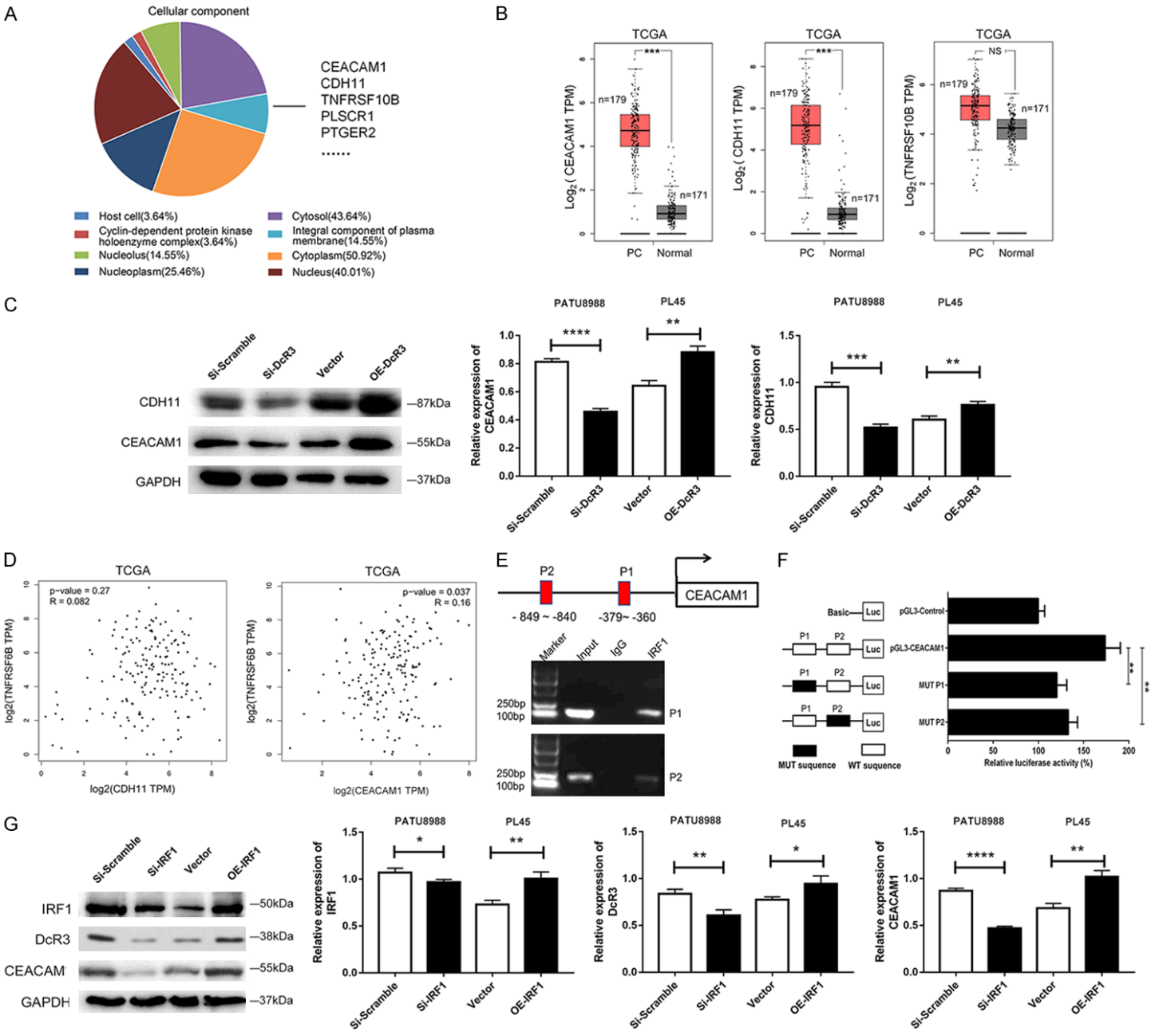
A
Cellular component
CEACAM1
CDH11
TNFRSF10B
PLSCR1
PTGER2
.....
Host cell(3.64%)
Cyclin-dependent protein kinase holoenzyme complex(3.64%)
Nucleolus(14.55%)
Nucleoplasm(25.46%)
Cytosol(43.64%)
Integral component of plasma membrane(14.55%)
Cytoplasm(50.92%)
Nucleus(40.01%)
B
TCGA
Log2 (CEACAM1 TPM)
Log2 (CDH11 TPM)
Log2 (TNFRSF10B TPM)
n=179
n=171
PC
Normal
NS
C
Si-Scramble
Si-DcR3
Vector
OE-DcR3
CDH11
CEACAM1
GAPDH
—87kDa
—55kDa
—37kDa
PATU8988
PL45
Relative expression of CEACAM1
Relative expression of CDH11
D
TCGA
p−value = 0.27
R = 0.082
p−value = 0.037
R = 0.16
log2(TNFRSF6B TPM)
log2(CDH11 TPM)
log2(CEACAM1 TPM)
E
P2
P1
CEACAM1
- 849 ~ -840
-379~ -360
Marker
Input
IgG
IRF1
250bp
100bp
F
Basic
Luc
pGL3-Control
pGL3-CEACAM1
MUT P1
MUT P2
MUT suquence
WT suquence
Relative luciferase activity (%)
G
Si-IRF1
OE-IRF1
IRF1
DcR3
CEACAM
—50kDa
—38kDa
—55kDa
—37kDa
Relative expression of IRF1
Relative expression of DcR3
Relative expression of CEACAM1

Figure 6. The relationship between DcR3 and CEACAM1. A. Cellular component analysis showed that 8 plasma membrane proteins were correlated with DcR3. B. TCGA database showed that CEACAM1 and CDH11 were upregulated in pancreatic cancer tissues (n=179) compared with control (n=171) (****P*<0.001) while TNFRSF10B showed no significant difference between the two groups (*P*>0.05). Mann-Whitney test was used to analyze the differences between groups, data were presented as the median with range. C. Western blot assays showed changes in the levels of CEACAM1 and CDH11 in DcR3 knockdown or DcR3-overexpressing cells. D. DcR3 TPM was associated with CEACAM1 TPM (**P*=0.037) but not with CDH11 (*P*=0.27) in TCGA database. E. ChIP assay showed PCR products targeting P1-P2 of the CEACAM1 promoter. Specific anti-IRF1 or control normal mouse IgG was used for immunoprecipitations, whereas genomic DNA was used as the input control. F. Luciferase assay showed that IRF1 could bind to the two CEACAM1 promoter sites. G. Western blot was used to examine the expression of DcR3 and CEACAM1 after manipulating IRF1 expression. The data were represented as the mean ± S.D. of three independent experiments in vitro. Significant differences are indicated as follows: *P<0.05, **P<0.01, ***P<0.001 and ****P<0.0001.

STAT signalling pathway was activated by DcR3 based on KEGG analysis. Second, the interaction network was centred on STAT1/STAT2, NF-κB, IFN-α/IFN-β, IRF1, and IRF7. Third, our experimental data suggested that DcR3 could enhance the phosphorylation levels of STAT1 and STAT2.

STAT1, a member of the STAT family, is a signal transduction and transcriptional activation factor protein that is involved in the development of cancer [26]. Interestingly, STAT1 has both tumour suppressive and tumour promotive activity [27-29]. The antitumour properties of STAT1 correlate with an increase in the expression of pro-apoptotic caspase genes and inhibition of the expression of bcl-xl and bcl-2. Contrary to its antitumour effects, STAT1 increases the transcriptional activity of cyclin D1 to promote tumour proliferation in hepatocellular carcinoma [30]. Other studies have also demonstrated the ability of STAT1 to increase PI3K/AKT/mTOR signalling and promote the survival of KRAS colon tumours [31, 32]. In the present study, our results provided evidence that DcR3 promoted the proliferation and invasion of pancreatic cancer cells, at least, partially through STAT1 activation.

In addition, we found that STAT1 transactivated IRF1 and that activation of IRF1 stimulated the expression and transcriptional activity of DcR3 and CEACAM1. IRF1, which belongs to the interferon regulatory factor family, was initially characterized as a transcriptional activator. Members of this family were originally recognized for their roles in inflammatory responses; however, recent research has suggested that they are also involved in tumor biology [33]. Other recent studies have demonstrated that IRF1 gene induction by IFN-γ was consistent with its rapid transactivation by phospho-Y701-STAT1 [34]. Meanwhile, IRF1 is characterized as a transcriptional regulator, serving as an activator of genes involved in cell proliferation, apoptosis, the immune response, and DNA damage response [35]. In our study, we also predicted a potential binding site of IRF1 within the DcR3 promoter. ChIP and luciferase assays showed that IRF1 directly bound the DcR3 promoter. Therefore, DcR3, STAT1 and IRF1 formed a positive feedback loop. DcR3 expression was reinforced by this positive feedback loop in the latency pathway, permitting even higher production, and ultimately promoting tumour cell growth and invasion.

Finally, we found that CEACAM1, a plasma membrane protein, was regulated by DcR3. CEACAM1 mediates cell adhesion via homophilic and heterophilic binding to other proteins [36]. Previous studies found that increased CEACAM1 expression significantly contributed to many human malignant tumours, including breast cancer [37], colorectal cancer [38], and pancreatic cancer [39]. In the present study, IRF1 activated by DcR3 increased the transcriptional activity of CEACAM1 by binding to the CEACAM1 promoter in pancreatic cancer cells. However, further studies will be required to define the precise molecular mechanism of the regulation of CEACAM1 by DcR3.

In summary, our results demonstrated that DcR3 promoted the phosphorylation of STAT1, leading to a dramatic increase in IRF1. IRF1 then increased the transcriptional activity of DcR3, forming a positive feedback loop to reinforce DcR3 and CEACAM1 expression. Therefore, we have not only illuminated a molecular mechanism underlying the regulation of DcR3 in pancreatic cancer cells but also have revealed that the new DcR3/STAT1/IRF1 feedback loop is a promising therapeutic strategy for pancreatic cancer.

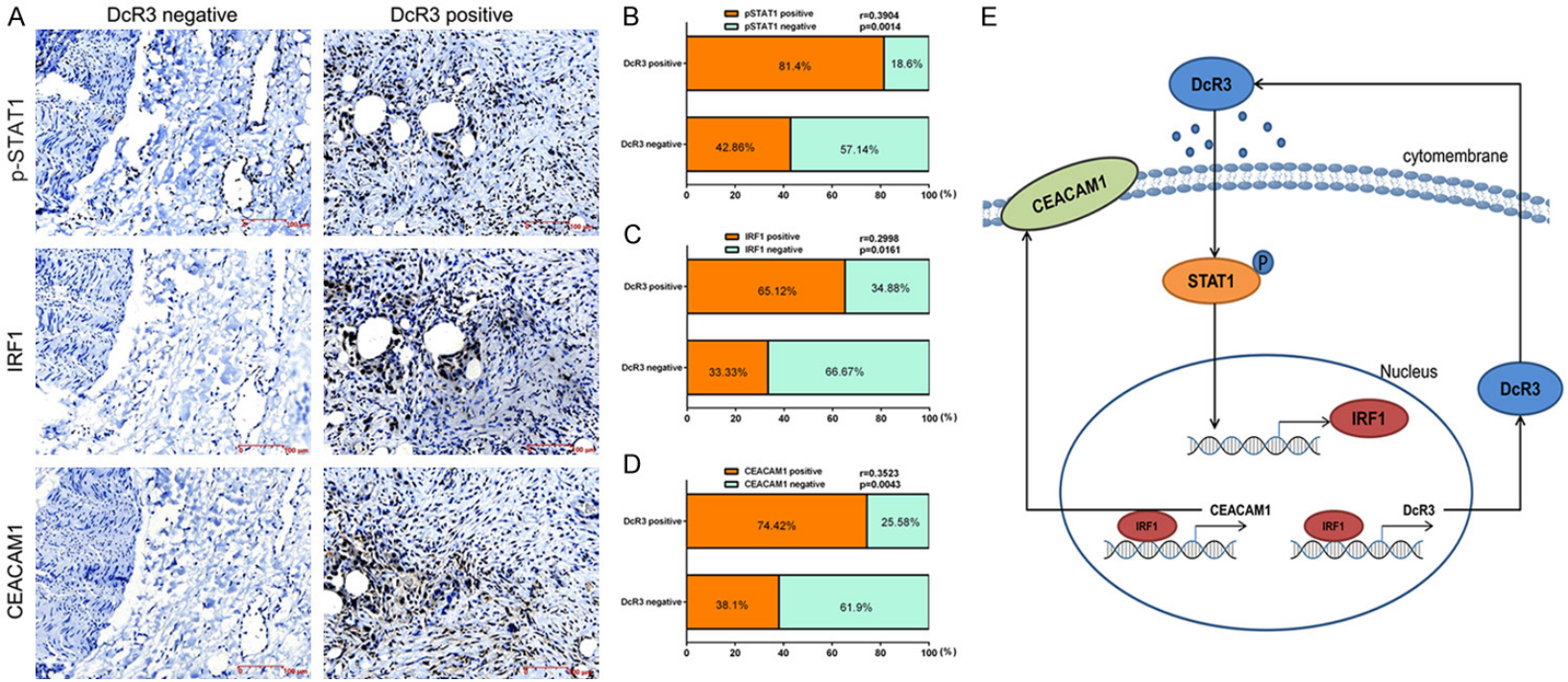

Figure 7. Relationship between DcR3/STAT1/IRF1 and CEACAM1 in pancreatic cancer tissues. A. IHC for p-STAT1, IRF1 and CEACAM1 was performed between DcR3 negative group (left panel) and DcR3 positive group (right panel) in 64 pancreatic cancer tissue samples. Representative cases show stains of the same cohorts of pancreatic cancer sections. Magnification ×100. B-D. Correlation analysis of the expression of DcR3 with that of p-STAT1 (r=0.3904, ***P*=0.0014), IRF1 (r=0.2998, **P*=0.0161) and CEACAM1 (r=0.3523, ***P*=0.0043). E. Schematic illustration showing that DcR3/STAT1/IRF1 forms a feedback loop to reinforce DcR3 and CEACAM1 expression.

Acknowledgements

This study was supported by the Project of Key Research and Development of Jiangsu Province of P. R. China (BE2016673), Jiangsu Provincial Medical Youth Talent (QNRC2016734), Jiangsu Provincial Six Talent Peaks project (WSW-059), Jiangsu Provincial "333" project (BRA2018392) and the Project of Medical Research of Jiangsu Province (Y2018094).

Disclosure of conflict of interest

None.

Address correspondence to: Dongming Zhu and Jian Zhou, Pancreatic Disease Research Centre, The First Affiliated Hospital of Soochow University, Suzhou 215006, Jiangsu, China. Tel: +86-0512-67780107; E-mail: sd310@126.com (DMZ); zhoujian06@suda.edu.cn (JZ)

References

[1] Siegel RL, Miller KD and Jemal A. Cancer statistics, 2018. CA Cancer J Clin 2018; 68: 7-30.

[2] Kamisawa T, Wood LD, Itoi T and Takaori K. Pancreatic cancer. Lancet 2016; 388: 73-85.

[3] Polireddy K and Chen Q. Cancer of the pancreas: molecular pathways and current advancement in treatment. J Cancer 2016; 7: 1497-514.

[4] Karagiannis GS, Pavlou MP and Diamandis EP. Cancer secretomics reveal pathophysiological pathways in cancer molecular oncology. Mol Oncol 2010; 4: 496-510.

[5] Schaaij-Visser TB, de Wit M, Lam SW and Jiménez CR. The cancer secretome, current status and opportunities in the lung, breast and colorectal cancer context. Biochim Biophys Acta 2013; 1834: 2242-58.

[6] Villarreal L, Méndez O, Salvans C, Gregori J, Baselga J and Villanueva J. Unconventional secretion is a major contributor of cancer cell line secretomes. Mol Cell Proteomics 2013; 12: 1046-60.

[7] Grønborg M, Kristiansen TZ, Iwahori A, Chang R, Reddy R, Sato N, Molina H, Jensen ON, Hruban RH, Goggins MG, Maitra A and Pandey A. Biomarker discovery from pancreatic cancer secretome using a differential proteomic approach. Mol Cell Proteomics 2006; 5: 157-71.

[8] Mustafa S, Pan L, Marzoq A, Fawaz M, Sander L, Rückert F, Schrenk A, Hartl C, Uhler R, Yildirim A, Strobel O, Hackert T, Giese N, Büchler MW, Hoheisel JD and Alhamdani MS. Comparison of the tumor cell secretome and patient sera for an accurate serum-based diagnosis of pancreatic ductal adenocarcinoma. Oncotarget 2017; 8: 11963-11976.

[9] Pitti RM, Marsters SA, Lawrence DA, Roy M, Kischkel FC, Dowd P, Huang A, Donahue CJ, Sherwood SW, Baldwin DT, Godowski PJ, Wood WI, Gurney AL, Hillan KJ, Cohen RL, Goddard AD, Botstein D and Ashkenazi A. Genomic amplification of a decoy receptor for Fas ligand in lung and colon cancer. Nature 1998; 396: 699-703.

[10] Zhang Y, Luo J, He R, Huang W, Li Z, Li P, Dang Y, Chen G and Li S. Expression and clinicopathological implication of DcR3 in lung cancer tissues: a tissue microarray study with 365 cases. Onco Targets Ther 2016; 9: 4959-68.

[11] Hu R, Liu W, Qiu X, Lin Z, Xie Y, Hong X, Paerhati R, Qi Z, Zhuang G and Liu Z. Expression of tumor necrosis factor-alpha-induced protein 8 in stage III gastric cancer and the correlation with DcR3 and ERK1/2. Oncol Lett 2016; 11: 1835-1840.

[12] Ge H, Liang C, Li Z, An D, Ren S, Yue C and Wu J. DcR3 induces proliferation, migration, invasion, and EMT in gastric cancer cells via the PI3K/AKT/GSK-3beta/beta-catenin signaling pathway. Onco Targets Ther 2018; 11: 4177-4187.

[13] Chen J, Guo XZ, Li HY, Zhao JJ and Xu WD. Dendritic cells engineered to secrete anti-DcR3 antibody augment cytotoxic T lymphocyte response against pancreatic cancer in vitro. World J Gastroenterol 2017; 23: 817-829.

[14] Wang W, Zhang M, Sun W, Yang S, Su Y, Zhang H, Liu C, Li X, Lin L, Kim S, Okunieff P, Zhang Z and Zhang L. Reduction of decoy receptor 3 enhances TRAIL-mediated apoptosis in pancreatic cancer. PLoS One 2013; 8: e74272.

[15] Yu W, Xu YC, Tao Y, He P, Li Y, Wu T, Zhu YP, Li J, Wu JX and Dai J. DcR3 regulates the growth and metastatic potential of SW480 colon cancer cells. Oncol Rep 2013; 30: 2741-8.

[16] Liang QL, Wang BR and Li GH. DcR3 and survivin are highly expressed in colorectal carcinoma and closely correlated to its clinicopathologic parameters. J Zhejiang Univ Sci B 2009; 10: 675-82.

[17] Zhao T, Xu Y, Ren S, Liang C, Zhou X and Wu J. The siRNA silencing of DcR3 expression induces fas ligand-mediated apoptosis in HepG2 cells. Exp Ther Med 2018; 15: 4370-4378.

[18] Ma Z, Wang B, Wang M, Sun X, Tang Y, Li M, Li F and Li X. TL1A increased IL-6 production on fibroblast-like synoviocytes by preferentially activating TNF receptor 2 in rheumatoid arthritis. Cytokine 2016; 83: 92-98.

[19] del Rio ML, Fernandez-Renedo C, Chaloin O, Scheu S, Pfeffer K, Shintani Y, Perez-Simon JA, Schneider P and Rodriguez-Barbosa JI. Immunotherapeutic targeting of LIGHT/LTbetaR/

HVEM pathway fully recapitulates the reduced cytotoxic phenotype of LIGHT-deficient T cells. MAbs 2016; 8: 478-90.
[20] Zhang Y, Li D, Zhao X, Song S, Zhang L, Zhu D, Wang Z, Chen X and Zhou J. Decoy receptor 3 suppresses fasL-induced apoptosis via ERK1/2 activation in pancreatic cancer cells. Biochem Biophys Res Commun 2015; 463: 1144-51.
[21] Liu YP, Zhu HF, Liu DL, Hu ZY, Li SN, Kan HP, Wang XY and Li ZG. DcR3 induces epithelial-mesenchymal transition through activation of the TGF-beta3/SMAD signaling pathway in CRC. Oncotarget 2016; 7: 77306-77318.
[22] Li J, Xie N, Yuan J, Liu L, Zhou Q, Ren X, Chen Q, Zhang G, Ruan Q, Chen YH and Wan X. DcR3 combined with hematological traits serves as a valuable biomarker for the diagnosis of cancer metastasis. Oncotarget 2017; 8: 107612-107620.
[23] Ge H, Liang C, Ren S, Yue C and Wu J. Prognostic value of DcR3 in solid tumors: a meta-analysis. Clin Chim Acta 2018; 481: 126-131.
[24] Hsieh SL and Lin WW. Decoy receptor 3: an endogenous immunomodulator in cancer growth and inflammatory reactions. J Biomed Sci 2017; 24: 39.
[25] Jin Z, Liu S, Zhan Q, Shao X, Ma J and Pan L. Decoy receptor 3 alleviates hepatic fibrosis through suppressing inflammation activated by NF-kappaB signaling pathway. Adv Clin Exp Med 2018; 27: 441-447.
[26] Ivashkiv LB. IFNgamma: signalling, epigenetics and roles in immunity, metabolism, disease and cancer immunotherapy. Nat Rev Immunol 2018; 18: 545-558.
[27] Josahkian JA, Saggioro FP, Vidotto T, Ventura HT, Candido Dos Reis FJ, de Sousa CB, Tiezzi DG, de Andrade JM, Koti M and Squire JA. Increased STAT1 expression in high grade serous ovarian cancer is associated with a better outcome. Int J Gynecol Cancer 2018; 28: 459-465.
[28] Crnčec I, Modak M, Gordziel C, Svinka J, Scharf I, Moritsch S, Pathria P, Schlederer M, Kenner L, Timelthaler G, Müller M, Strobl B, Casanova E, Bayer E, Mohr T, Stöckl J, Friedrich K and Eferl R. STAT1 is a sex-specific tumor suppressor in colitis-associated colorectal cancer. Mol Oncol 2018; 12: 514-528.
[29] Kaowinn S, Kaewpiboon C, Koh SS, Krämer OH and Chung YH. STAT1HDAC4 signaling induces epithelialmesenchymal transition and sphere formation of cancer cells overexpressing the oncogene, CUG2. Oncol Rep 2018; 40: 2619-2627.
[30] Huang J, Zheng C, Shao J, Chen L, Liu X and Shao J. Overexpression of eEF1A1 regulates G1-phase progression to promote HCC proliferation through the STAT1-cyclin D1 pathway. Biochem Biophys Res Commun 2017; 494: 542-549.
[31] Wang S, Darini C, Désaubry L and Koromilas AE. STAT1 promotes KRAS colon tumor growth and susceptibility to pharmacological inhibition of translation initiation factor eIF4A. Mol Cancer Ther 2016; 15: 3055-3063.
[32] Chew GS, Myers S, Shu-Chien AC and Muhammad TS. Interleukin-6 inhibition of peroxisome proliferator-activated receptor alpha expression is mediated by JAK2- and PI3K-induced STAT1/3 in HepG2 hepatocyte cells. Mol Cell Biochem 2014; 388: 25-37.
[33] Yang G, Zhang S, Gao F, Liu Z, Lu M, Peng S, Zhang T and Zhang F. Osteopontin enhances the expression of HOTAIR in cancer cells via IRF1. Biochim Biophys Acta 2014; 1839: 837-48.
[34] Trilling M, Le VT, Rashidi-Alavijeh J, Katschinski B, Scheller J, Rose-John S, Androsiac GE, Jonjic S, Poli V, Pfeffer K and Hengel H. "Activated" STAT proteins: a paradoxical consequence of inhibited JAK-STAT signaling in cytomegalovirus-infected cells. J Immunol 2014; 192: 447-58.
[35] Dou L, Liang HF, Geller DA, Chen YF and Chen XP. The regulation role of interferon regulatory factor-1 gene and clinical relevance. Hum Immunol 2014; 75: 1110-4.
[36] Gray-Owen SD and Blumberg RS. CEACAM1: contact-dependent control of immunity. Nat Rev Immunol 2006; 6: 433-46.
[37] Yang C, He P, Liu Y, He Y, Yang C, Du Y, Zhou M, Wang W, Zhang G, Wu M and Gao F. Assay of serum CEACAM1 as a potential biomarker for breast cancer. Clin Chim Acta 2015; 450: 277-81.
[38] Ieda J, Yokoyama S, Tamura K, Takifuji K, Hotta T, Matsuda K, Oku Y, Nasu T, Kiriyama S, Yamamoto N, Nakamura Y, Shively JE and Yamaue H. Re-expression of CEACAM1 long cytoplasmic domain isoform is associated with invasion and migration of colorectal cancer. Int J Cancer 2011; 129: 1351-61.
[39] Simeone DM, Ji B, Banerjee M, Arumugam T, Li D, Anderson MA, Bamberger AM, Greenson J, Brand RE, Ramachandran V and Logsdon CD. CEACAM1, a novel serum biomarker for pancreatic cancer. Pancreas 2007; 34: 436-43.

Table S1. The ChIP primers of gene promoter

Site	Primers	bp
The primers of IRF1 gene promoter		
P1	F: 5'-AGGTTTGGCATTGGTCACA-3'	134 bp
	R: 5'-TGCAGGCTATAAATAGACACACC-3'	
P2	F: 5'-GTGAAGGAAATGACACGCC-3'	122 bp
	F: 5'-CCTAGAGACTTGACTGGGTGTT-3'	
The primers of DcR3 gene promoter		
P1	F: 5'-GCCTATAAGCAAGACGACGA-3'	176 bp
	F: 5'-GGAGCTTCAATCAGACCCG-3'	
The primers of CEACAM1 gene promoter		
P1	F: 5'-GCTTTGCTAAGGAGGTGAAGG-3'	132 bp
	F: 5'-ACAGGGACCCCTCACAGAAC-3'	
P2	F: 5'-ACCTGAGACCCCTGGACTTG-3'	174 bp
	F: 5'-TTCAGTGTGCTGGGAAGGTAG-3'	

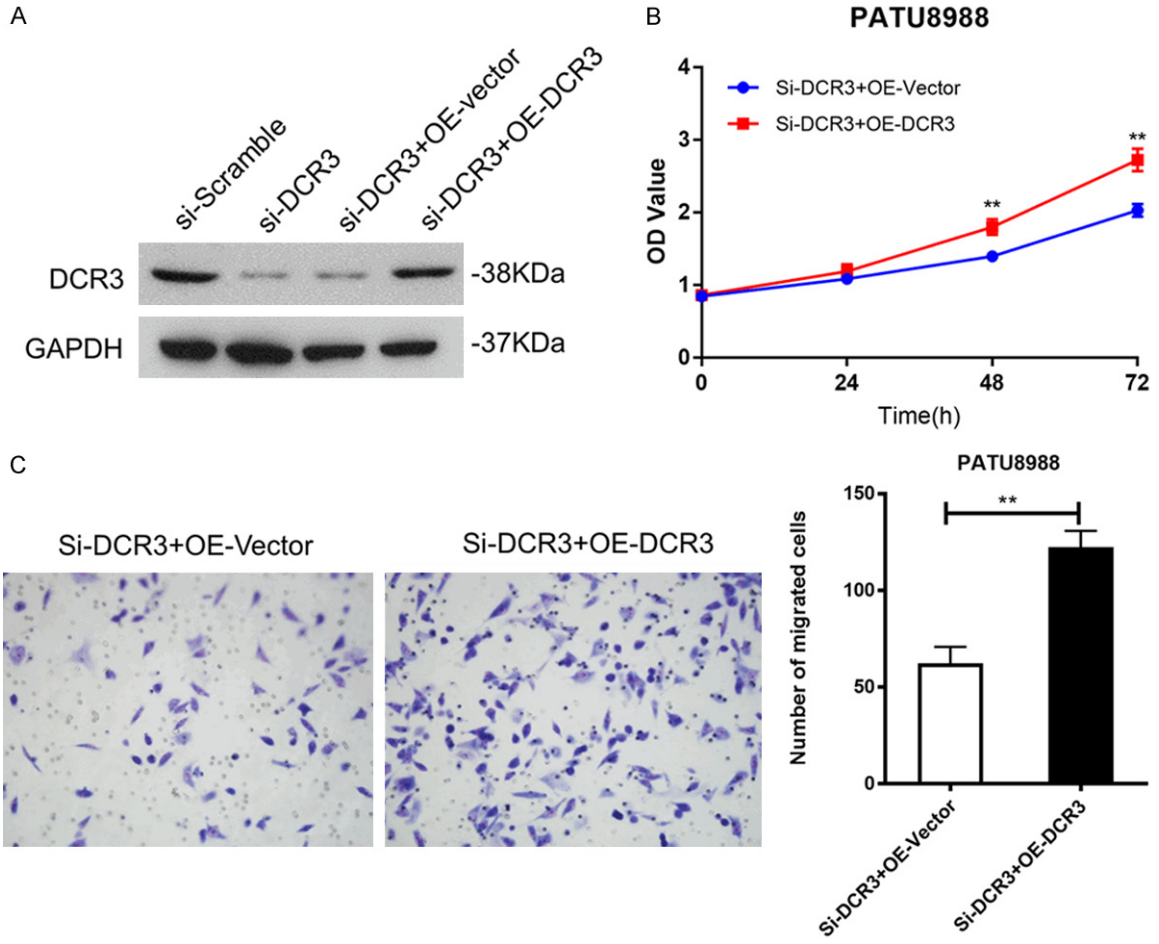

Figure S1. A rescue experiment for siRNA experiments. A. We first silenced DcR3 expression by RNAi and then up-regulated DcR3 expression by pcDNA3.1-DcR3. Western blot assays showed changes in the levels of DcR3. GAPDH was used as a loading control. B. Growth curves were determined via CCK8 assays. C. DcR3 promoted PC cell invasion based on Transwell assays. The data were represented as the mean ± S.D. of three independent experiments. Significant differences are indicated as follows: **P<0.01.

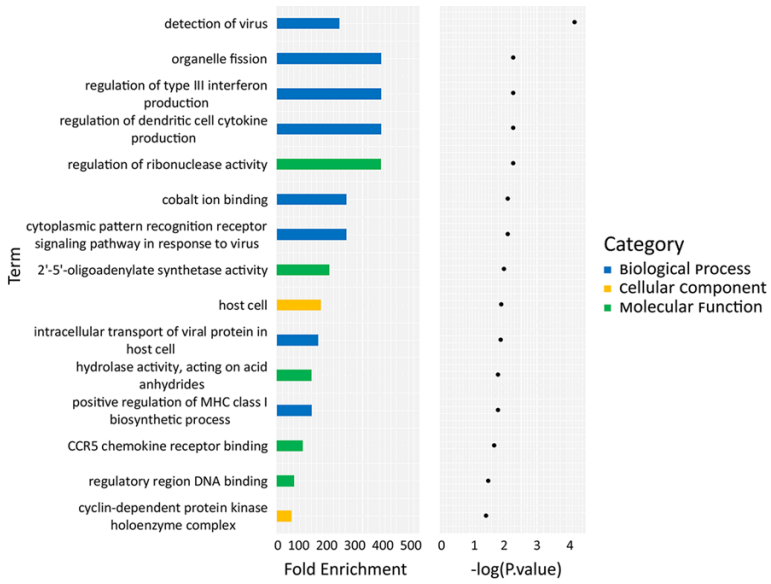

Figure S2. Gene Ontology (GO) analysis indicated genes regulated by DcR3 were involved in Biological Process (BP), Cellular Component (CC) and Molecular Function (MF). P<0.05.